Self-Similar Theory of Thermal Conduction and Application to the Solar Wind

K. Horaites,[1] S. Boldyrev,[1] S. I. Krasheninnikov,[2] C. Salem,[3] S. D. Bale,[3,4] and M. Pulupa[3]
[1]*Department of Physics, University of Wisconsin, Wisconsin-Madison 53706, USA*
[2]*Department of Mechanical and Aerospace Engineering, University of California San Diego, La Jolla, California 92093, USA*
[3]*Space Sciences Laboratory, University of California, Berkeley, California 94720, USA*
[4]*Department of Physics, University of California, Berkeley, California 94720, USA*
(Received 20 March 2015; published 18 June 2015)

We propose a self-similar kinetic theory of thermal conductivity in a magnetized plasma, and discuss its application to the solar wind. We study a collisional kinetic equation in a spatially expanding magnetic flux tube, assuming that the magnetic field strength, the plasma density, and the plasma temperature decline as power laws of distance along the tube. We demonstrate that the electron kinetic equation has a family of scale-invariant solutions for a particular relation among the magnetic-, density-, and temperature-scaling exponents. These solutions describe the heat flux as a function of the temperature Knudsen number γ, which we require to be constant along the flux tube. We observe that self-similarity may be realized in the solar wind; for the Helios data 0.3–1 AU we find that the scaling exponents for density, temperature, and heat flux are close to those dictated by scale invariance. We find steady-state solutions of the self-similar kinetic equation numerically, and show that these solutions accurately reproduce the electron strahl population seen in the solar wind, as well as the measured heat flux.

DOI: 10.1103/PhysRevLett.114.245003 PACS numbers: 52.25.Xz, 52.25.Dg, 95.30.Qd, 96.50.Ci

Introduction.—In a plasma where $f(\mathbf{v})$ is the local electron velocity distribution function, the heat flux $\mathbf{q} = \int (mv^2/2)\mathbf{v} f d^3v$ describes the flow of electron kinetic energy [1]. Solving for $\mathbf{q}$ in terms of other bulk plasma parameters (density, temperature) is important for understanding energy transport. In studies of the solar wind, the heat flux is often prescribed as a step in obtaining profiles for the solar wind speed [2,3], as a player in the steady-state global energy balance [4], and as a source of free energy that drives instabilities [5].

Spitzer and Härm [6] solved the kinetic equation for $f(\mathbf{v})$ in the presence of a temperature gradient, using perturbation theory. This yielded an expression for the heat flux in the absence of a net electric current:

$$q_{sh} = -\kappa_{\parallel} \nabla_{\parallel} T. \tag{1}$$

Here $\kappa_{\parallel} \propto T^{5/2}$ is the thermal conductivity parallel to the magnetic field.

The Spitzer-Härm relation applies for collisional plasmas, where the collisional mean free path λ_{mfp} is sufficiently small. The degree of collisionality is parametrized by the temperature Knudsen number:

$$\gamma = -T^2 (d \ln T/dx)/(2\pi e^4 \Lambda n) \sim \lambda_{mfp}/L_T, \tag{2}$$

where $L_T = |d \ln T/dx|^{-1}$, Λ is the electron Coulomb logarithm, and x is the direction of the temperature variation. If $\gamma \ll 1$, the plasma is *collisional* and Eq. (1) applies, otherwise it is *weakly collisional* or *collisionless* and the description of $\mathbf{q}$ becomes more complicated. In particular, the Spitzer-Härm expansion is formally valid for $\gamma \lesssim 0.01$, while for larger values a population of "thermal runaway" electrons may contribute to the heat flux [e.g., [7,8]]. Thus in a plasma with a temperature gradient, a population of electrons is locally detected that originated from distant, hotter regions. In the limiting case $\gamma \gtrsim 1$ the collisionless or "free-streaming" heat flux is given by the thermal energy density advected at the thermal speed, $q \sim n v_{th} T$ [7,9].

Laboratory and astrophysical applications, however, require modeling the heat flux outside the limiting cases discussed above. For example, the authors of [10] proposed a formula, $q(x) = \int q_{sh}(x') w(x, x') dx'$, that is widely used in the laser-plasma interaction community [see, e.g., [11–13]]. The kernel $w(x, x')$ is a phenomenological expression chosen so as to give results that match with Fokker-Planck simulations of a weakly collisional plasma. A more rigorous but mathematically involved approach [14] employed a simplified kinetic equation in a 1D spatial geometry, and expanded the perturbation from a Maxwellian distribution in orthogonal polynomials. In recent years, kinetic models of the solar corona and the solar wind have been developed that include the effects of Coulomb collisions [15–19]. In these models, detailed radial profiles of the bulk plasma parameters are prescribed, and the distribution function is found numerically.

Recent measurements of the electron distribution function made by the Wind satellite's electrostatic analyzers EESA-L and EESA-H [20] have revealed a functional relationship between q and γ in the range of Knudsen numbers $0.01 \lesssim \gamma \lesssim 1$, where the analytic treatment of the heat flux is especially complicated. This suggests that γ is the fundamental parameter needed to predict the heat flux and the electron distribution function in the weakly collisional solar wind.

In this work, we propose that the kinetic equation in a magnetized plasma, where the large-scale parameters (temperature, density, and magnetic field) exhibit power-law behavior, has scale-invariant "self-similar" solutions. These solutions are more transparent physically and easier to construct numerically than standard perturbative solutions. The requirement of scale invariance dictates that $\gamma = \text{const}$, a condition that is also consistent with solar wind measurements.

The self-similar kinetic theory of heat conduction was first proposed in [8], which allowed for calculation of the electron distribution function in a nonmagnetic one-dimensional case $T = T(x)$, $n = n(x)$ [21]. A class of self-similar steady-state solutions of the kinetic equation was found in the form

$$f(\mathbf{v}, x) = NF(\mathbf{v}/v_{th}(x))/T(x)^{\alpha}, \tag{3}$$

where N is a constant set by the normalization $\int f(\mathbf{v})d^3v = n$, $\int F(\mathbf{u})d^3u = 1$. The parameter α depends on the relative scaling of density and temperature.

In this work, we develop a 3D self-similar kinetic theory that includes a spatially expanding magnetic field $\mathbf{B} = B(x)\hat{x}$. We obtain the electron distribution function and the heat flux as functions of the Knudsen number γ, and demonstrate that they are in good agreement with solar wind measurements. Our results provide an effective new way of modeling electron physics in weakly collisional astrophysical and space plasmas.

Self-similar kinetic equation for magnetized plasma.— Consider a cylindrically symmetric magnetic flux tube, expanding along the $\hat{x}$ direction. When the plasma collision rate is much smaller than the gyrofrequency, the time evolution of the electron distribution function f is governed by the drift kinetic equation [see, e.g., [22]]. We assume the $\mathbf{E} \times \mathbf{B}$ drift is negligible for the transport along the flux tube. We also neglect the solar wind velocity v_{sw}, since we are interested in a weakly collisional case, $\gamma \gtrsim 0.01$, when significant contribution to the heat flux comes from the energetic electrons $v \gtrsim v_{th} \gg v_{sw}$. The drift kinetic equation can now be written in terms of t, x, v, μ ($\mu = \mathbf{v} \cdot \hat{x}/v$), and the collision operator $\hat{C}(f)$:

$$\frac{\partial f}{\partial t} + \mu v \frac{\partial f}{\partial x} - \frac{1}{2}\frac{d\ln B}{dx} v(1-\mu^2)\frac{\partial f}{\partial \mu} - \frac{eE_{\parallel}}{m}\left[\frac{1-\mu^2}{v}\frac{\partial f}{\partial \mu} + \mu\frac{\partial f}{\partial v}\right] = \hat{C}(f). \tag{4}$$

We now assume power-law variations of physical parameters in the x direction: $B \propto x^{\alpha_B}$, $n \propto x^{\alpha_n}$, $T \propto x^{\alpha_T}$. It can be checked that the equation has a self-similar form in the case $\gamma(x) \equiv \text{const}$. In what follows we are interested in the steady-state case $\partial f/\partial t = 0$. As a result, Eq. (4) can be rewritten in terms of the two dimensionless variables μ and $\xi = (v/v_{th})^2 \equiv mv^2/(2T)$:

$$-\gamma\left[\alpha\mu F + \mu\xi\frac{\partial F}{\partial \xi} + \frac{\alpha_B}{2}(\alpha + 1/2)(1-\mu^2)\frac{\partial F}{\partial \mu}\right] + \gamma_E\left[\mu\frac{\partial F}{\partial \xi} + \frac{1-\mu^2}{2\xi}\frac{\partial F}{\partial \mu}\right] + \hat{C}(F) = 0, \tag{5}$$

where $\gamma_E = E_{\parallel}eT/(2\pi e^4\Lambda n)$. Although the Landau collision operator can also be written in a self-similar form, for simplicity we use the linearized collision operator, valid for $\xi \gg 1$, defining $\beta \equiv (1 + Z_{\text{eff}})/2$ for background ions with total effective charge Z_{eff} [23–25]:

$$\hat{C}(F) = \frac{1}{\xi}\left[\frac{\partial F}{\partial \xi} + \frac{\partial^2 F}{\partial \xi^2}\right] + \frac{\beta}{2\xi^2}\frac{\partial}{\partial \mu}(1-\mu^2)\frac{\partial F}{\partial \mu}. \tag{6}$$

The terms in $\hat{C}(F)$ with derivatives of ξ are due to energy exchange with the thermal electrons, while the terms with derivatives of μ describe pitch angle scattering from the thermal electrons and ions. The requirements $\gamma = \text{const}$ and the self-similar form of f [Eq. (3)] give the following restriction for the allowed scaling powers α, α_n, and α_T:

$$\alpha = \frac{3}{2} - \frac{\alpha_n}{\alpha_T} = \frac{1}{\alpha_T} - \frac{1}{2}. \tag{7}$$

Interestingly, this relation has a solution $n \propto x^{-2}$ and $T \propto x^{-1/2}$, which also implies $q \propto x^{-11/4}$ [[8], Eq. (5)]. Such profiles are close to the typically measured variations of n, T, q with heliospheric distance [26–28].

Runaway electrons.—The presence of density and temperature gradients in a magnetized plasma leads to the formation of a runaway electron population (see, for example, [7]). A spatially expanding magnetic field focuses this population into a narrow field-aligned beam. In the limit $\mu \approx 1$, $\xi \gg 1$ we approximate $(1-\mu^2) \approx 2(1-\mu)$, and neglect the energy exchange terms in the collision operator. With the definitions $z = \xi^2(1-\mu)$, $\eta = \ln\xi$, $\alpha' = [2-(\alpha+1/2)\alpha_B]$, and $F = \phi(\eta, z)$, Eq. (5) reduces to

$$\gamma\alpha\phi + \gamma\frac{\partial \phi}{\partial \eta} + \{\gamma\alpha' z - \beta\}\frac{\partial \phi}{\partial z} = \beta z\frac{\partial^2 \phi}{\partial z^2}. \tag{8}$$

The solution of this advection-diffusion-type equation has the form:

$$F(\xi, \mu) \sim C\xi^{\alpha'-\alpha}\exp\left\{\frac{\gamma\alpha'\xi^2(1-\mu)}{\beta}\right\}, \tag{9}$$

where the constant C can be found from matching with the full solution at $\xi \sim 1$. The full solution is constructed numerically in the next section.

Numerical solution.—Equation (5) can be solved once the two parameters of the system, α and α_B, are specified. This equation has an important subfamily of solutions that can be found numerically in a nonperturbative fashion. We use the method of relaxation and add to the left-hand side of Eq. (5) a time-dependent term $\xi^{-1/2}\partial F/\partial\tau$. We then would like to view the time-dependent Eq. (5) as a formal Fokker-Planck equation of some stochastic process (see, e.g., [29]). This is possible to do if the norm of the function is preserved, $\int F\sqrt{\xi}d\mu d\xi = \text{const}$. The norm preservation leads to the extra condition on the allowed parameters, $\alpha_B = (2-\alpha)/(\alpha+1/2)$, which defines the one-parameter subfamily of solutions.

For a particular illustration, consider a radially expanding magnetic flux tube, say modeling the inner heliosphere, with $\alpha_B = -2$. In this case, the other scaling exponents are found as $\alpha = -3$, and $\alpha_n = -1.8$, $\alpha_T = -0.4$, which are roughly consistent with power laws observed in the solar wind, as discussed in previous sections. Defining the function $\psi(\mu,\xi,\tau) \equiv \xi^{1/2}F$, the evolution equation can be rewritten as

$$\frac{\partial\psi}{\partial\tau} = \frac{\partial}{\partial\xi}\left[-\gamma\mu\xi^{3/2}\psi + \gamma_E\mu\sqrt{\xi}\psi + \frac{\psi}{\sqrt{\xi}}\right] + \frac{\partial}{\partial\mu}\left\{\left[-\frac{5}{2}\gamma(1-\mu^2)\sqrt{\xi} + \frac{\gamma_E(1-\mu^2)}{2\sqrt{\xi}} + \frac{\beta\mu}{\xi^{3/2}}\right]\psi\right\} + \frac{\partial^2}{\partial\xi^2}\frac{\psi}{\sqrt{\xi}} + \frac{\partial^2}{\partial\mu^2}\left[\frac{\beta(1-\mu^2)}{2\xi^{3/2}}\psi\right]. \tag{10}$$

The function ψ can be constructed using the Langevin method. In this method, the $\mu-\xi$ phase space is populated by a large number of points, each evolving according to the stochastic ordinary differential equations:

$$\frac{d\xi}{d\tau} = \gamma\mu\xi^{3/2} - \gamma_E\mu\sqrt{\xi} - \frac{1}{\sqrt{\xi}} + \frac{\sqrt{2}}{\xi^{1/4}}\nu_\xi(\tau), \tag{11}$$

$$\frac{d\mu}{d\tau} = \frac{5}{2}\gamma(1-\mu^2)\sqrt{\xi} - \frac{\gamma_E(1-\mu^2)}{2\sqrt{\xi}} - \frac{\beta\mu}{\xi^{3/2}} + \frac{\sqrt{\beta(1-\mu^2)}}{\xi^{3/4}}\nu_\mu(\tau), \tag{12}$$

where $\nu_\xi(\tau)$, $\nu_\mu(\tau)$ are normally distributed independent random variables (random noises) with mean of zero and standard deviation of $\langle\nu_\xi(\tau)\nu_\xi(\tau')\rangle = \langle\nu_\mu(\tau)\nu_\mu(\tau')\rangle = \delta(\tau-\tau')$. Equations (11)–(12) are solved using the forward Euler finite-difference method with the Ito prescription for the noise discretization [29], setting $\beta = 1$. The electric field γ_E is adjusted at each time step so as to nullify the current $\int^{\xi_{max}}\psi\mu\xi^{1/2}d\xi d\mu$, where we choose $\xi_{max} >> 1$, see "Discussion and Conclusions. The function $\psi(\mu,\xi)$ is approximated by a 2D histogram of the points in phase space with the normalization $\pi\int\psi(\mu,\xi)d\xi d\mu = 1$. The simulation is initialized with a Gaussian distribution, and a quasi-steady state is reached at time $\tau\sim 1$, whose amplitude decreases very slowly afterwards in the region $\xi < \xi_{max}$.

Applications to the solar wind.—The solar wind electron velocity distribution function (eVDF) was measured at heliocentric distances 0.3–1 AU by the E1 plasma experiment onboard the Helios 1 satellite [30]. We fit each eVDF in our data set to a function $f_m(v_\perp, v_\parallel) = f_c + f_h + f_s$, which represents a sum of the well-known core, halo, and strahl subpopulations [26]. We adopt a bi-Maxwellian f_c, bi-kappa f_h [31], and a modified bi-kappa function f_s that is diminished on one side [32]. We disallow perpendicular bulk drifts, $v_{\perp,c} = v_{\perp,h} = v_{\perp,s} = 0$. Our fitting procedure is described in detail in [33].

For each measured Helios eVDF, γ is computed from Eq. (2), where T and n are the core values T_c, n_c obtained from the least-squares fit. Since the parallel and perpendicular core temperatures may differ, we define $T \equiv T_c = (T_{c\parallel} + 2T_{c\perp})/3$. In order to calculate dT/dx from our measurements, we must prescribe how x varies with heliocentric distance r. We assume that the flux tube follows the average Parker spiral: $x(r) = \int dr/\cos\theta_P$, where $\tan\theta_P(r) = r/r_0$ and $r_0 = 1$ AU [34]. We can then fit a power law to our observed $T(x)$, which yields $\alpha_T = -0.6 \pm 0.1$. To verify our assumption $\gamma \approx \text{const}$, we plot a 2D histogram of γ versus r in Fig. 1. At all distances 0.3–1 AU the most probable value is $\gamma \approx 0.2$.

In Fig. 2, we plot parallel and perpendicular cuts of the distribution function obtained from the Helios data and from our solution. Because the E1 detector has a broad field of view, it tends to smear out narrow features in the distribution function such as the strahl; we denote the resulting convoluted (self-similar) function as $F^*(\mathbf{v}/v_{th})$. In order to model F^* using our numerical solution F of Eq. (5), we apply the convolution $F^* = [\int R(\phi,\theta)Fd\Omega]/\int R(\phi,\theta)d\Omega$, where $R(\phi,\theta) = [H(\phi+\Delta\phi) - H(\phi-\Delta\phi)]\exp\{-[(\theta-\pi/2)/\Delta\theta]^2\}$ and H is the Heaviside

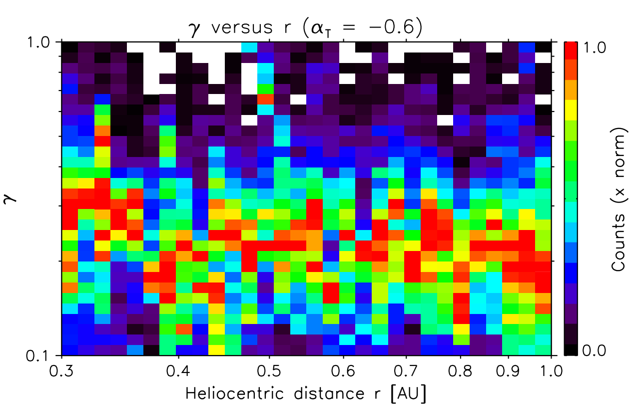

FIG. 1 (color online). 2D histogram of γ versus heliocentric distance r, derived from fits to Helios eVDF data. Each column is normalized by its peak, to bring out the functional dependence. We observe $\gamma(r) \approx \text{const}$, required in order to apply the self-similar theory.

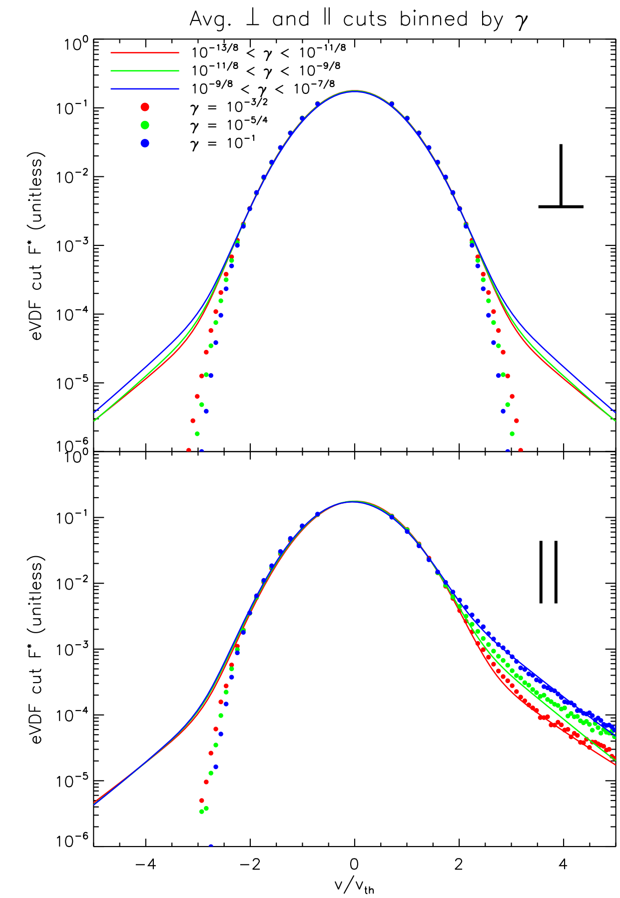

FIG. 2 (color online). Perpendicular and parallel cuts of F^* from the Helios measurements (lines) and Langevin simulations (dots). The Helios data are averaged into logarithmically spaced bins $10^{-13/8} < \gamma < 10^{-7/8}$. The numerical solutions are found with γ chosen at the logarithmic center of a bin.

step function. Here ϕ and θ are spherical coordinates in the Helios spacecraft frame, where the rotation axis defines the z direction; the nominal look direction of the detector ($\mu = 1, 0$ for parallel, perpendicular cuts) corresponds with $\phi = 0$, $\theta = \pi/2$. In accordance with the detector description [26], we set $\Delta\phi = 15°$, $\Delta\theta = 11.4°$. We plot cuts of F^* from the numerical solution of our model as dots in Fig. 2, for $\gamma = 10^{-3/2}, 10^{-5/4}, 10^{-1}$.

The function F^* is computed from each observed Helios distribution function f_m using $F^*(\mathbf{v}/v_{th}) = f_m(\mathbf{v})v_{th}^3/n$ (note that $N = nT^\alpha/v_{th}^3$, from the normalization of F). We take the parallel and perpendicular cuts of F^* obtained from our fits to the Helios data, and average them into three logarithmically spaced bins in the interval $10^{-13/8} < \gamma < 10^{-7/8}$. These are plotted as lines in Fig. 2. We see good agreement between the data and theory in the core, as should be expected, but also a striking agreement in the strahl population. The halo population appears not to be described by our solutions.

The recent results of [20], which demonstrate the transition between the Spitzer-Härm-like and collisionless heat flux regimes in the solar wind at 1 AU, are reproducible with the Helios data measured 0.3–1 AU. We adopt the same definitions: $q_0 = (3/2)nv_{th}T$ [35], $q_{sh} = 3.16nT\tau_e/m$ [6,36], $q_{sh}/q_0 = 1.07\lambda_{mfp}/L_T = 2.84\gamma$ [37]. We plot a 2D histogram of the variation of q/q_0 with λ_{mfp}/L_T in Fig. 3. For reference, we show the Spitzer-Härm-like scaling as a solid line.

The dots in Fig. 3 are predictions of our model. For each steady-state distribution F, a dimensionless heat flux can be calculated $Q \equiv \int u_\parallel u^2 F(\mathbf{u})d^3u$, where $\mathbf{u} = \mathbf{v}/v_{th}$. From our definitions it can be quickly derived $q/q_0 = 2Q/3$. Using this and $\lambda_{mfp}/L_T = 2.656\gamma$ gives the coordinates of the dots in Fig. 3. Our theory is consistent with the heat flux measurements.

Discussion and conclusions.—We have demonstrated that in a magnetic flux tube where $\gamma(x) = \mathrm{const}$ and the density, temperature, and magnetic fields vary as power laws, the steady-state electron kinetic equation admits solutions $F(\mu, \xi)$ that depend on just two self-similar variables. We found that the electron distribution functions measured by the Helios satellite closely match many of the predictions of our theory. Most notably, the theory is able to describe the transition from the Spitzer-Härm-like to the collisionless regime, recently observed by [20] in the interval $0.01 \lesssim \gamma \lesssim 1$. It also shows that the strahl population consists of thermal runaway electrons that originated from hotter, denser regions, which are focused by the magnetic field. We note that the halo population does not follow the self-similar solution; it is observed to vary in a non-self-similar fashion in the inner heliosphere, while self-similarity is a better approximation for the strahl (Fig. 5 in [31]), (Fig. 6 in [32]). Physics beyond the scope of this Letter may be required to explain the halo.

For finite systems, it is necessary to restrict the domain of self-similarity to a range in energy $\xi < \xi_{\max}$, since runaway

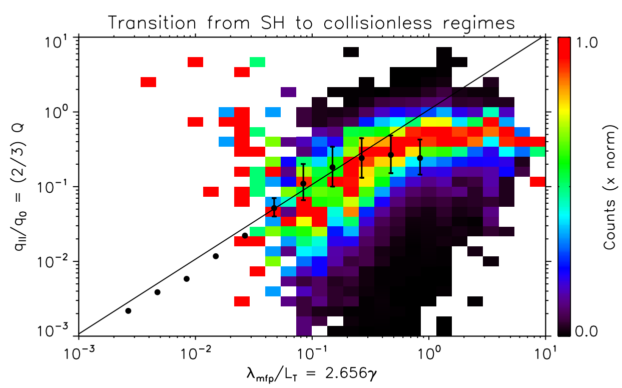

FIG. 3 (color online). 2D histogram of q/q_0 versus heliocentric distance λ_{mfp}/L_T, derived from fits to Helios eVDF data, correcting for the Parker spiral angle and assuming $\alpha_T = -2/5$. Each column is normalized by its peak, to bring out the functional dependence. The Spitzer-Härm prediction is shown as a line. Results of our numerical solutions are shown as dots.

strahl electrons can only be supplied up to energies comparable to the thermal energy at the higher temperature boundary (such an effect may be witnessed in the simulations of [18], Fig. 5). Restricting the self-similar energy domain is also necessary from a theoretical standpoint [8]: multiplying Eq. (9) with $\mu\xi^{3/2}$ and integrating up to infinite energies, we find that the heat flux formally diverges for our assumed parameters. The temperatures at the coronal base are about 20 times higher than in the solar wind at 1 AU. We set $\xi_{\max} = 50$ when calculating q in Fig. 3, which realistically captures the extent of the strahl observed by Helios. For comparison, the upper and lower error bars indicate the heat flux computed by using $\xi_{\max} = 100$ and $\xi_{\max} = 25$, respectively.

In general, Eq. (5) admits a two-parameter family of solutions, parametrized by the scaling exponent of the magnetic field and the temperature along the flux tube. Depending on these parameters, other solutions may provide a better match to different laboratory or astrophysical systems. We plan to study the solutions of Eq. (5) in fuller generality elsewhere.

This research was supported by the NSF Center for Magnetic Self-Organization in Laboratory and Astrophysical Plasmas at the University of Wisconsin-Madison, by the U. S. DOE Award No. DE-SC0003888, by the NASA Grant No. NNX11AE12G, and by the National Science Foundation under Grants No. NSF PHY11-25915 and No. AGS-1261659. S. B. appreciates the hospitality and support of the Kavli Institute for Theoretical Physics, University of California, Santa Barbara, where part of this work was performed.

[1] We will only consider electrons here, and drop the species subscript by default.

[2] E. N. Parker, Astrophys. J. **128**, 664 (1958).
[3] B. D. G. Chandran, T. J. Dennis, E. Quataert, and S. D. Bale, Astrophys. J. **743**, 197 (2011).
[4] E. Marsch and A. K. Richter, J. Geophys. Res. **89**, 6599 (1984).
[5] S. P. Gary, E. E. Scime, J. L. Phillips, and W. C. Feldman, J. Geophys. Res. **99**, 23391 (1994).
[6] L. Spitzer and R. Härm, Phys. Rev. **89**, 977 (1953).
[7] A. V. Gurevich and Y. N. Istomin, Soviet J. Exp. Theor. Phys. **50**, 470 (1979).
[8] S. I. Krasheninnikov, JETP **67**, 2483 (1988).
[9] E. N. Parker, Astrophys. J. **139**, 93 (1964).
[10] J. F. Luciani, P. Mora, and J. Virmont, Phys. Rev. Lett. **51**, 1664 (1983).
[11] E. M. Epperlein and R. W. Short, Phys. Fluids B **3**, 3092 (1991).
[12] G. P. Schurtz, P. D. Nicolaï, and M. Busquet, Phys. Plasmas **7**, 4238 (2000).
[13] C. D. Sijoy, S. Chaurasia, V. Mishra, P. Leshma, N. Sakthivel, S. Chaturvedi, S. M. Sharma, and S. Basu, High Energy Density Phys. **11**, 36 (2014).
[14] E. D. Held, J. D. Callen, C. C. Hegna, and C. R. Sovinec, Phys. Plasmas **8**, 1171 (2001).
[15] Ø. Lie-Svendsen, V. H. Hansteen, and E. Leer, J. Geophys. Res. **102**, 4701 (1997).
[16] V. Pierrard, M. Maksimovic, and J. Lemaire, J. Geophys. Res. **106**, 29305 (2001).
[17] S. Landi, L. Matteini, and F. Pantellini, Astrophys. J. **760**, 143 (2012).
[18] H. M. Smith, E. Marsch, and P. Helander, Astrophys. J. **753**, 31 (2012).
[19] S. Landi, L. Matteini, and F. Pantellini, Astrophys. J. Lett. **790**, L12 (2014).
[20] S. D. Bale, M. Pulupa, C. Salem, C. H. K. Chen, and E. Quataert, Astrophys. J. Lett. **769**, L22 (2013).
[21] I. F. Potapenko and S. I. Krasheninnikov, J. Plasma Phys. **77**, 803 (2011).
[22] R. M. Kulsrud, in *Basic Plasma Physics: Selected Chapters, Handbook of Plasma Physics, Volume 1*, edited by A. A. Galeev and R. N. Sudan (North Holland Publishing Company, Amsterdam, 1983), p. 1.
[23] S. I. Braginskii, Rev. Plasma Phys. **1** (1965).
[24] S. P. Hirshman and D. J. Sigmar, Phys. Fluids **19**, 1532 (1976).
[25] S. I. Krasheninnikov and O. G. Bakunin, Contributions Plasma Phys. **32**, 255–260 (1993).
[26] W. G. Pilipp, K.-H. Muehlhaeuser, H. Miggenrieder, M. D. Montgomery, and H. Rosenbauer, J. Geophys. Res. **92**, 1075 (1987).
[27] E. Marsch, K. M. Thieme, H. Rosenbauer, and W. G. Pilipp, J. Geophys. Res. **94**, 6893 (1989).
[28] M. Maksimovic, S. P. Gary, and R. M. Skoug, J. Geophys. Res. **105**, 18337 (2000).
[29] J. Zinn-Justin, *Quantum Field Theory and Critical Phenomena*, 4th ed. (Oxford University Press, Oxford, 2002).
[30] R. Schwenn, H. Rosenbauer, and H. Miggenrieder, Raumfahrtforschung : DGRR-Journal **19**, 226 (1975).
[31] M. Maksimovic, I. Zouganelis, J.-Y. Chaufray, K. Issautier, E. E. Scime, J. E. Littleton, E. Marsch, D. J. McComas, C. Salem, R. P. Lin, and H. Elliott, J. Geophys. Res. **110**, A09104 (2005).
[32] Š. Štverák, M. Maksimovic, P. M. Trávníček, E. Marsch, A. N. Fazakerley, and E. E. Scime, J. Geophys. Res. **114**, A05104 (2009).
[33] K. Horaites, C. Salem, S. D. Bale, and M. Pulupa (unpublished).
[34] J. G. Luhmann, T.-L. Zhang, S. M. Petrinec, C. T. Russell, P. Gazis, and A. Barnes, J. Geophys. Res. **98**, 5559 (1993).
[35] A. J. Hundhausen, *Coronal Expansion and Solar Wind* (Springer-Verlag, Berlin and Heidelberg, Germany); Physics and Chemistry in Space (1972), Vol. 5.
[36] J. Huba, U.S.O. of Naval Research, and N.R.L. (U.S.), NRL Plasma Formulary, NRL publication (Naval Research Laboratory, 1998).
[37] C. Salem, D. Hubert, C. Lacombe, S. D. Bale, A. Mangeney, D. E. Larson, and R. P. Lin, Astrophys. J. **585**, 1147 (2003).